K-space and Image Space Combination for Motion-induced Phase Error Correction in 3D Diffusion-Weighted Imaging

A. T. Van[1], D. C. Karampinos[2,3], and B. P. Sutton[1,4]

[1]Electrical and Computer Engineering, University of Illinois, Urbana, IL, United States, [2]Mechanical Science and Engineering, University of Illinois, Urbana, IL, United States, [3]Beckman Institute, University of Illinois, Urbana, IL, United States, [4]Bioengineering, University of Illinois, Urbana, IL, United States

INTRODUCTION In diffusion tensor imaging (DTI), high-resolution isotropic voxels are highly desirable to resolve small white matter structures. Isotropic voxels require high spatial resolution including the slice direction and can only be achieved with reasonable SNR with 3D diffusion-weighted imaging (DWI). A major problem with 3D DWI is motion-induced phase errors (MiP). Recently, 3D self-navigated interleave spiral (SNAILS) was introduced to correct for MiP [1]. 3D SNAILS is time demanding in image correction and reconstruction. In this work, we developed a new MiP correction for 3D DWI based on the previously developed method of *k*-space and image space combination (KICT) for rigid body MiP correction in 2D DWI [2]. Both simulation and in vivo results show the effectiveness of the correction method in removing MiP, resulting in high-quality, high-resolution 3D diffusion-weighted images.

METHOD The main challenges when moving from 2D DWI to 3D DWI include designing a time efficient 3D trajectory with 3D navigators, estimating and correcting the resulting 3D phase errors, and reconstructing images in 3D.

The 3D trajectory used in this study is a stack of multishot spirals and a low resolution, fully-sampled, stack of single shot spirals is acquired at the beginning of each shot for 3D navigating purposes. The stack of spirals trajectory is used because it is simple to implement and facilitates fast processing of the navigator data (2D gridding in-plane and 1D FFT through plane). For each application of diffusion gradients, a single shot in only one plane of the stack is acquired.

To estimate and correct for motion-induced phase errors, we extend the 2D model for MiP for rigid body motion developed by Anderson and Gore to 3D case

$$\tilde{M}(k_x,k_y,k_z) = e^{j\varphi_e} M\left(k_x+\Delta k_x, k_y+\Delta k_y, k_z+\Delta k_z\right) \quad (1)$$

$$\tilde{I}(x,y,z) = e^{j\left[\varphi_e + 2\pi\left(x(k_x+\Delta k_x)+y(k_y+\Delta k_y)+z(k_z+\Delta k_z)\right)\right]} I(x,y,z) \quad (2)$$

where $\tilde{M}$ is the corrupted 3D *k*-space data, *M* is the ideal 3D *k*-space data, $\tilde{I}$ is the corrupted 3D image, *I* is the ideal 3D image, φ_e is the constant phase offset, and Δk_x, Δk_y, Δk_z are *k*-space shifts in k_x, k_y and k_z directions, respectively [3]. From equation (1), MiP caused by rigid body motion can be corrected by shifting the 3D *k*-space trajectory and multiplying the corrupted *k*-space data by the conjugate of the constant phase offset. From equation (2), similar to the 2D KICT, for each shot on each plane of the stack of spirals, MiP is estimated as the difference of the phases between $b \neq 0$ and the reference $b = 0$ images reconstructed from 3D navigator data [2]. The phase errors are then unwrapped and least squares fitted to a linear function to get the *k*-space shifts. The phase offset, φ_e , is estimated as the phase of the peak *k*-space data point.

Because the correction for motion-induced phase errors involves shifting of the *k*-space trajectory, the resulting trajectory for the DWI dataset is no longer a stack of spirals. Therefore, fast reconstruction with 2D gridding in-plane and 1D FFT through plane is not applicable. Instead, a 3D gridding algorithm is implemented. The algorithm uses a 3D separable Kaiser-Bessel kernel with the parameters that provide the least relative aliased energy as given in [4]. Sampling density function $\rho(k_x, k_y, k_z)$ is computed as [4]

$$\rho\left(k_x,k_y,k_z\right) = S\left(k_x,k_y,k_z\right) * C\left(k_x,k_y,k_z\right) \quad (3)$$

where *S* denotes the sampling function, and *C* is the 3D convolution kernel.

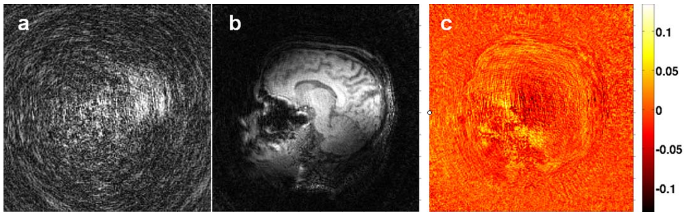

Fig 1. 3D reconstruction of simulated data: (a) uncorrected, (b) corrected, (c) normalized difference between corrected and simulated phantom.

RESULTS Simulation The chosen 3D DWI trajectory and motion-induced phase error correction algorithm was tested using a 3D structural image as a numerical phantom. Matrix size of the phantom is 190x190x160 with a field of view (FOV) of 30 cm. Random errors are applied to individual shots and correspond to constant phase offsets in *U(-π, π)* and *k*-space shifts in *U(-3/FOV, 3/FOV)*. Fig. 1 shows reconstructed images with and without motion-induced phase error correction. The uncorrected image is highly corrupted by the errors. The corrected image restores the simulated phantom. The residual errors come from the locally under-sampled *k*-space trajectory resulting from the MiP correction.

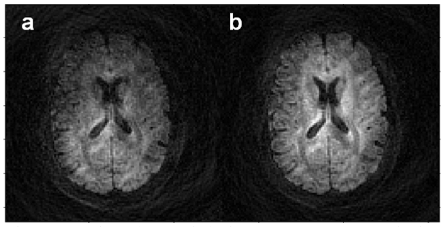

Fig. 2. In vivo data axial view: (a) uncorrected, (b) corrected

In vivo A 3D diffusion-weighted spin echo sequence was used to acquire in vivo data on a healthy male subject in accordance with the institutional review board. Data were acquired with a matrix size of 128x128x20 with a FOV of 24 x 24 x 4 cm on the level of corpus-callosum. TR 1 s, TE 58 ms. Diffusion encoding was performed in the [1 1 1] direction with a *b*-value of 770 s/mm^2, $\delta = 22$ ms, $\Delta = 32$ ms, and $g = 30$ mT/m. The 3D trajectory was 16-shot in-plane spirals and 20 equidistant z-planes. Regional saturation is applied to suppress the signal from outside of the volume of interest. Fig. 2 and Fig. 3 compare the uncorrected and corrected in vivo data in axial, sagital and coronal view. The corrected images give large improvement in the image quality. The total time for phase error estimation and image reconstruction is 6 minutes on an Intel Core 2 2.66Ghz with 2GB RAM. For comparison, in 3D SNAILS, the reported time to correct and reconstruct a 128 x 128 x 128 volume is 1~3 hours if direct phase subtraction is used and more than 22 hours if conjugate-gradient iterative method is used [1].

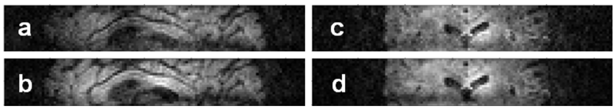

Fig. 3. In vivo data sagital and coronal view: (a) sagital uncorrected, (b) sagital corrected, (c) coronal uncorrected, (d) coronal corrected.

DISCUSSION In 3D SNAILS, because the MiP correction is performed in 3D image space, a 3D volume of *k*-space data has to be acquired in a single application of diffusion gradients, resulting in prolonged gradient readouts. To keep short gradient readouts, a single shot in only one plane of the stack is acquired in the present method.

The correction procedure in the new method involves shifting of the *k*-space trajectory. Therefore, it is possible that the resulting *k*-space is locally under-sampled. However, Bracewell has showed that irregularly-sampled data can be correctly reconstructed even when local regions do not satisfy Nyquist [5]. In our experiments, we can still get high quality reconstruction even with the large shifts of five *k*-space points (5/FOV). An improvement of image quality can be obtained for much larger *k*-space shifts by combining the acquisition with parallel imaging or by acquiring the same set of data multiple times if there is flexibility in data acquisition time [6].

Finally, while gradient echo sequences are usually chosen for whole-brain coverage in 3D diffusion-weighted experiments, we selected spin echo sequence to image a certain volume of interest. Spin echo sequence allows the application of high *b*-value, which results in better diffusion-weighted images but at the cost of increased MiP. Furthermore, a spin echo sequence gives images that are immune to field inhomogeneity induced signal losses.

CONCLUSION A new MiP correction method for 3D DWI is presented. The method is more time efficient as compared to 3D SNAILS. This time efficiency comes from a simple 3D acquisition strategy, and phase error model. As shown by both simulation and in vivo data, the new correction method gives high quality 3D diffusion-weighted images, which are highly desired in DTI.

REFERENCES [1] Zhang et al., 15th ISMRM; [2] Van et al., EMBC 08; [3] Anderson et al., MRM, 32, 379-387; [4] Jackson et al., TMI, 10, 473-478; [5] Bracewell, New York: McGraw-Hill, 1986; [6] Atkinson et al., MRM, 44, 101-109.